Atmospheric Environment 84 (2014) 254–261

Contents lists available at ScienceDirect

Atmospheric Environment

journal homepage: www.elsevier.com/locate/atmosenv

Improved monitoring of surface ozone by joint assimilation of geostationary satellite observations of ozone and CO

Peter Zoogman [a,*], Daniel J. Jacob [a,b], Kelly Chance [c], Helen M. Worden [d], David P. Edwards [d], Lin Zhang [a,1]

[a] Department of Earth and Planetary Sciences, Harvard University, Cambridge, MA, United States
[b] School of Engineering and Applied Sciences, Harvard University, Cambridge, MA, United States
[c] Harvard Smithsonian Center for Astrophysics, Cambridge, MA, United States
[d] National Center for Atmospheric Research, Boulder, CO, United States

HIGHLIGHTS

- We implement a joint data assimilation for concurrent ozone and CO observations.
- Ozone–CO model error correlations are positive over ocean but negative over land.
- Geostationary measurement of CO provides substantial benefit for monitoring ozone.

ARTICLE INFO

Article history:
Received 25 July 2013
Received in revised form
18 November 2013
Accepted 21 November 2013

Keywords:
Ozone
Kalman filter
CO
Joint assimilation
Error correlation
Remote sensing

ABSTRACT

Future geostationary satellite observations of tropospheric ozone aim to improve monitoring of surface ozone air quality. However, ozone retrievals from space have limited sensitivity in the lower troposphere (boundary layer). Data assimilation in a chemical transport model can propagate the information from the satellite observations to provide useful constraints on surface ozone. This may be aided by correlated satellite observations of carbon monoxide (CO), for which boundary layer sensitivity is easier to achieve. We examine the potential of concurrent geostationary observations of ozone and CO to improve constraints on surface ozone air quality through exploitation of ozone–CO model error correlations in a joint data assimilation framework. The hypothesis is that model transport errors diagnosed for CO provide information on corresponding errors in ozone. A paired-model analysis of ozone–CO error correlations in the boundary layer over North America in summer indicates positive error correlations in continental outflow but negative regional-scale error correlations over land, the latter reflecting opposite sensitivities of ozone and CO to boundary layer depth. Aircraft observations from the ICARTT campaign are consistent with this pattern but also indicate strong positive error correlations in fine-scale pollution plumes. We develop a joint ozone–CO data assimilation system and apply it to a regional-scale Observing System Simulation Experiment (OSSE) of the planned NASA GEO-CAPE geostationary mission over North America. We find substantial benefit from joint ozone–CO data assimilation in informing US ozone air quality if the instrument sensitivity for CO in the boundary layer is greater than that for ozone. A high-quality geostationary measurement of CO could potentially relax the requirements for boundary layer sensitivity of the ozone measurement. This is contingent on accurate characterization of ozone–CO error correlations. A finer-resolution data assimilation system resolving the urban scale would need to account for the change in sign of the ozone–CO error correlations between urban pollution plumes and the regional atmosphere.

© 2013 Elsevier Ltd. All rights reserved.

1. Introduction

Ozone in surface air is harmful to humans and vegetation. 129 million people in the United States (US) breathe hazardous levels of ozone as measured by the National Ambient Air Quality Standard (NAAQS) of 75 ppb (maximum daily 8-h average not to be exceeded more than 3 times per year) (US Environmental Protection Agency

* Corresponding author. Present address: Harvard Smithsonian Center for Astrophysics, 60 Garden Street, Cambridge, MA 02138, United States. Tel.: +1 6174965414.
E-mail address: pzoogman@cfa.harvard.edu (P. Zoogman).
[1] Present address: Department of Atmospheric and Oceanic Sciences, School of Physics, Peking University, Beijing, China.

1352-2310/$ – see front matter © 2013 Elsevier Ltd. All rights reserved.
http://dx.doi.org/10.1016/j.atmosenv.2013.11.048

(EPA), 2012). Ozone is produced by photochemical oxidation of carbon monoxide (CO) and volatile organic compounds (VOCs) in the presence of nitrogen oxide radicals ($NO_x \equiv NO + NO_2$). The chemistry is complex and non-linear, making it difficult to relate ozone exceedances to precursor emissions. Satellite observations of ozone and its precursors show considerable promise for monitoring emissions and transport, as well as chemical regime (Martin, 2008), but direct observation of ozone air quality from space has been limited by poor sensitivity in the boundary layer. Here we show that combined ozone and CO measurements from a geostationary satellite platform can significantly increase the observational capability for ozone through data assimilation as compared to ozone measurements alone.

Ozone has major absorption features in the ultraviolet (UV) and the thermal infrared (TIR). These have provided the foundation for high-quality satellite retrievals of tropospheric ozone by the GOME and OMI instruments using UV solar backscatter (Liu et al., 2006, 2010b) and by the TES and IASI instruments using TIR terrestrial emission (Beer, 2006; Clerbaux et al., 2009). These instruments show good consistency between themselves and with ozonesondes (Zhang et al., 2010). However, they have poor sensitivity in the lower troposphere (boundary layer), in the UV because of molecular scattering and in the TIR because of lack of thermal contrast between the surface and lowermost atmospheric air temperatures. Multispectral observation in the UV, TIR, and in the weak visible (Vis) Chappuis bands may improve sensitivity in the boundary layer in the future (Natraj et al., 2011; Fu et al., 2013; Cuesta et al., 2013). In contrast to ozone, mature CO column observations from space with boundary layer sensitivity are available from solar backscatter in the near IR (NIR), as from the SCIAMACHY instrument (Bovensmann et al., 1999). The MOPITT satellite instrument has both NIR and TIR channels, enabling separation of boundary layer and free tropospheric CO (Worden et al., 2010).

CO is a product of incomplete combustion, with an atmospheric lifetime of about two months. It is a precursor of ozone, but more importantly it is a long-lived tracer of anthropogenic influence. Surface and aircraft observations in pollution plumes and continental outflow in summer show strong ozone–CO correlations and these have been used to test models of ozone production (Parrish et al., 1993, 1998; Chin et al., 1994; Hudman et al., 2009). Concurrent TIR observations of ozone and CO from TES in the free troposphere show strong summertime correlations at northern midlatitudes, reflecting continental outflow of ozone and intercontinental transport (Zhang et al., 2006, 2009; Hegarty et al., 2009, 2010; Voulgarakis et al., 2011). Kim et al. (2013) combined high-density satellite data of ozone from OMI (UV) and CO from AIRS (TIR) to show patterns of strong ozone–CO correlations (positive and negative) in the free troposphere over much of the world. Negative correlations are associated with air very remote from human influence or stratospheric intrusions.

Geostationary satellite measurements of atmospheric composition promise to revolutionize our observing system for air quality over the next decade (Fishman et al., 2012). They will provide continuous hourly data with ~5 km spatial resolution over continental scales, in contrast to the current fleet of low-elevation orbit satellites that have a return time of at most once per day. We anticipate a constellation of geostationary satellites from planned launches in the 2018–2020 time frame including TEMPO over North America (http://science1.nasa.gov/missions/tempo/), SENTINEL-4 over Europe (Ingmann et al., 2012), and GEMS over East Asia (Bak et al., 2013). They will include observation of ozone in the UV (SENTINEL-4, GEMS) and UV + Vis (TEMPO). Concurrent NIR and TIR measurements of CO and ozone from co-located satellites are presently under consideration, and in the case of North America these would largely complete the atmospheric component of GEO-CAPE (Geostationary Coastal And Pollution Events) (Fishman et al., 2012), a priority strategic mission for NASA recommended by the US National Research Council Decadal Survey (2007).

Observation System Simulation Experiments (OSSEs) in support of GEO-CAPE planning have demonstrated the theoretical capability of the mission for improved observation of surface ozone (Zoogman et al., 2011) and CO (Edwards et al., 2009) through data assimilation in a chemical transport model (CTM). In data assimilation, information from the observations is used to correct the CTM (referred to as the "forward model") on the fly and with appropriate weighting of model and measurement information based on their respective uncertainties. Even though the satellite instrument does not directly measure surface air concentrations, the CTM propagates the information from the observations to obtain an improved estimate of the 3-D concentration fields including surface values. Zoogman et al. (2011) showed that direct instrument sensitivity to the boundary layer (UV + Vis or UV + TIR channels) was necessary for GEO-CAPE to constrain surface ozone and then only with moderate success.

Here we examine whether improved estimates of surface ozone can be obtained from geostationary satellite observations through the constraint from ozone–CO error correlations in a joint assimilation of ozone and CO data. This may be particularly effective if satellite observations have more boundary layer sensitivity for CO than for ozone, as is currently the case. Diagnosed model error in simulating CO provides information on the coincident model error in simulating ozone. A similar idea has been used previously to improve CO_2 surface flux estimates through the use of combined CO_2 and CO observations together with CO_2–CO error correlations (Palmer et al., 2006; Wang et al., 2009). Statistics on ozone–CO error correlations are required, which may be different from the correlations in the concentrations themselves as pointed out by Wang et al. (2009).

Our OSSE framework involves the generation of synthetic ozone and CO data from a CTM to represent the "true" atmosphere. We use for that purpose the GEOS-Chem CTM v8-02-03 (Bey et al., 2001; http://www.geos-chem.org) driven by GEOS-5 assimilated meteorological data from the NASA Global Modeling and Assimilation Office (GMAO). We sample this 3-D field of ozone and CO "true" concentrations following the GEO-CAPE experimental design, with expected instrument errors, to mimic the observations that GEO-CAPE will provide. We then assimilate the resulting concentrations into a different GEOS-Chem CTM simulation driven by GEOS-4 meteorological data for the same period and taken as the forward model. From there we can assess the effectiveness of the GEO-CAPE observations to correct the forward model and reproduce the "true" concentration fields through data assimilation. The GEOS-4 and GEOS-5 meteorological data differ in the underlying general circulation model, the methodology for data assimilation, and the data assimilated (Bloom et al., 2005; Rienecker et al., 2008; Ott et al., 2009). In spite of their common heritage, GEOS-Chem simulations driven by GEOS-4 and GEOS-5 feature large differences for ozone and CO, as shown in previous studies (Liu et al., 2010a, 2013; Mitovski et al., 2012), and further illustrated below.

2. Joint ozone–CO data assimilation

A CTM generates a forecast of 3-D concentration fields at a given timestep by numerical integration from the previous timestep. We can reduce the forecast error by assimilating satellite observations over that timestep. The resulting optimized 3-D field of concentrations is called the *a posteriori* state. This *a posteriori* state is then evolved forward in time by the CTM until the next timestep, when we again assimilate observations. Data assimilation not only

enables improved forecasts of concentrations by correcting the successive initial conditions but also provides an optimal estimate of the state at any given time. We use here a Kalman filter where observations at discrete timesteps are used to optimize concentrations for the corresponding times, but our error correlation method is applicable to any Bayesian data assimilation technique. Previous applications of Kalman filters for assimilating ozone in a CTM have been presented by Khattatov et al. (2000) for the stratosphere and Parrington et al. (2008) for the troposphere.

Consider a nadir satellite instrument where retrieval of vertical concentration profiles from the radiance spectra is done by optimal estimation (Rodgers, 2000). Let **x** be the true vertical profile, i.e., the vector of true concentrations on a vertical grid. The retrieved profile **x'** is related to the true state **x** by the instrument averaging kernel matrix **A**, which gives the sensitivity of **x'** to **x** ($\mathbf{A}=\partial\mathbf{x}'/\partial\mathbf{x}$):

$$\mathbf{x}' = \mathbf{x}_S + \mathbf{A}(\mathbf{x} - \mathbf{x}_S) + \boldsymbol{\varepsilon} \quad (1)$$

where $\boldsymbol{\varepsilon}$ is the instrument noise vector and $\mathbf{x}_S$ is an independent *a priori* ozone profile used in the satellite retrieval process to constrain the solution.

In a single-species ozone assimilation we calculate an optimal *a posteriori* estimate $\hat{\mathbf{x}}$ of the ozone concentration at each observation timestep as an error-weighted average of the CTM forecast $\mathbf{x}_a$ (with error vector $\boldsymbol{\varepsilon}_a$ relative to the true profile) and the observations **x'**. The errors are characterized by error covariance matrices $\mathbf{S_a} = E[\boldsymbol{\varepsilon}_\mathbf{a}\boldsymbol{\varepsilon}_\mathbf{a}^T]$ and $\mathbf{S}\varepsilon = E[\boldsymbol{\varepsilon}\boldsymbol{\varepsilon}^T]$, where $E[\ ]$ is the expected-value operator. Assuming unbiased Gaussian distributions for $\varepsilon_\mathbf{a}$ and ε yields an analytical least-squares solution (Rodgers, 2000)

$$\hat{\mathbf{x}} = \mathbf{x}_a + \mathbf{G}\left(\mathbf{x}' - \mathbf{K}\mathbf{x}_a\right). \quad (2)$$

where **K** is the observation operator that maps the model state vector to the observation vector, including the vertical smoothing from the satellite retrieval and the interpolation from the model grid to the observation locations. The gain matrix **G** is given by

$$\mathbf{G} = \mathbf{S}_a\mathbf{K}^T\left(\mathbf{K}\mathbf{S}_a\mathbf{K}^T + \mathbf{S}_\varepsilon\right)^{-1}. \quad (3)$$

and determines the relative weight given to the observations and the model. The Kalman filter correction to the forecast concentrations is based on two terms: the gain matrix, which depends on the relative error in the model and the observations; and the innovation vector $\mathbf{x}'-\mathbf{K}\mathbf{x}_a$, which describes the mismatch between the observations and the model state.

In a joint ozone–CO assimilation we optimize ozone and CO concentrations simultaneously; the state vector is the concatenation of ozone and CO vertical profiles. The additional information from CO observations for optimizing the ozone concentrations is incorporated as covariance between model errors in ozone and CO concentrations. This covariance is described by off-diagonal terms in the model error covariance matrix $\mathbf{S_a}$, coupling the optimization of both species:

$$\mathbf{S}_a = \begin{pmatrix} \mathbf{S}_{a,O_3} & E\left[\boldsymbol{\varepsilon}_{a,O_3}\boldsymbol{\varepsilon}_{a,CO}^T\right] \\ E\left[\boldsymbol{\varepsilon}_{a,CO}\boldsymbol{\varepsilon}_{a,O3}^T\right] & \mathbf{S}_{a,CO} \end{pmatrix}. \quad (4)$$

where the subscripts O_3 and CO refer to the single-species errors, and $E[\boldsymbol{\varepsilon}_{a,O_3}\boldsymbol{\varepsilon}_{a,CO}^T] = E[\boldsymbol{\varepsilon}_{a,CO}\boldsymbol{\varepsilon}_{a,O_3}^T]$ is the covariance of the model errors. This covariance reflects the commonality of processes driving model error in both species; we will discuss in Section 3 its physical basis and the computation of its spatial variability. These coupled ozone–CO terms in the model error covariance matrix lead to corresponding terms in the gain matrix, which is then applied to the combined ozone–CO innovation vector. The optimal estimate of the ozone concentrations thus depends on the observation-model mismatch in both ozone and CO.

3. Characterizing ozone–CO error covariances

To perform a joint ozone–CO assimilation we must first derive the model error covariance matrix terms $E[\boldsymbol{\varepsilon}_{a,O_3}\boldsymbol{\varepsilon}_{a,CO}^T]$ for use in (4). The model error includes contributions from errors in emissions, chemistry, and transport. Relevant emission errors mainly involve NO_x (for ozone) and CO. Errors in NO_x and CO emissions are in general not correlated. Errors in chemistry are also not expected to be correlated, at least on the scale of polluted source regions where CO (with a chemical lifetime of months) can be considered inert. We therefore focus our attention on the correlation of transport errors.

To characterize the ozone–CO transport error correlation and its geographical distribution over North America we use the "paired-model" method (Wang et al., 2009) for August 2006. In the paired-model method we conduct GEOS-Chem CTM simulations of ozone and CO ($2^\circ\times2.5^\circ$ horizontal resolution) driven by different assimilated meteorological data sets, GEOS-4 and GEOS-5, for the same period. Since the GEOS-Chem CTM simulations are otherwise the same, the two simulations produce 3-D concentration fields of ozone and CO that differ only due to meteorology. The differences are substantial, as illustrated by the monthly mean surface values in Fig. 1. The differences in CO concentrations are 10–20%, typical of residual errors found when comparing model to observations after having optimized emissions (Heald et al., 2004; Kopacz et al., 2009).

Fig. 2 **(top)** shows the correlations between ozone and CO concentrations in the afternoon boundary layer (0–2 km, 1200–1700 local time) for August 2006. We find a positive correlation over most of North America and the western North Atlantic, consistent with observations (Parrish et al., 1993; Chin et al., 1994; Hudman et al., 2009). The correlation is strongest over the western North Atlantic, reflecting the contrast between North American outflow (high ozone, high CO) and clean marine air (low ozone, low CO).

Comparison of model results for the GEOS-4 and GEOS-5 simulations in each grid square generates time series of concentration differences, Δozone and ΔCO, where Δ means "difference between GEOS-4 and GEOS-5". Fig. 2 **(bottom)** shows the correlations between Δozone and ΔCO, i.e. the ozone–CO model error correlations, for the 0–2 km column. The Atlantic coastline marks a sharp boundary between negative and positive error correlations. We see that the error correlations are very different from the correlations between the concentrations themselves, as previously noted by Wang et al. (2009) for CO_2–CO correlations. Error correlations are positive over continental outflow regions and the West but negative over the East and South. We find no significant model error correlations above 2 km even though there are significant correlations in concentrations (Kim et al., 2013).

Examination of the meteorological data shows that the negative ozone–CO error correlations over the East and South in Fig. 2 are due to differences in daytime boundary layer depths between GEOS-4 and GEOS-5. A deeper boundary layer results in more entrainment from the free troposphere, which tends to have higher ozone and lower CO concentrations than surface air (Dawson et al., 2007). Model error in boundary layer depth thus leads to anti-correlated errors in ozone and CO concentrations. In outflow regions we find a positive error correlation due to the dominant effect of horizontal transport from source regions for both ozone and CO.

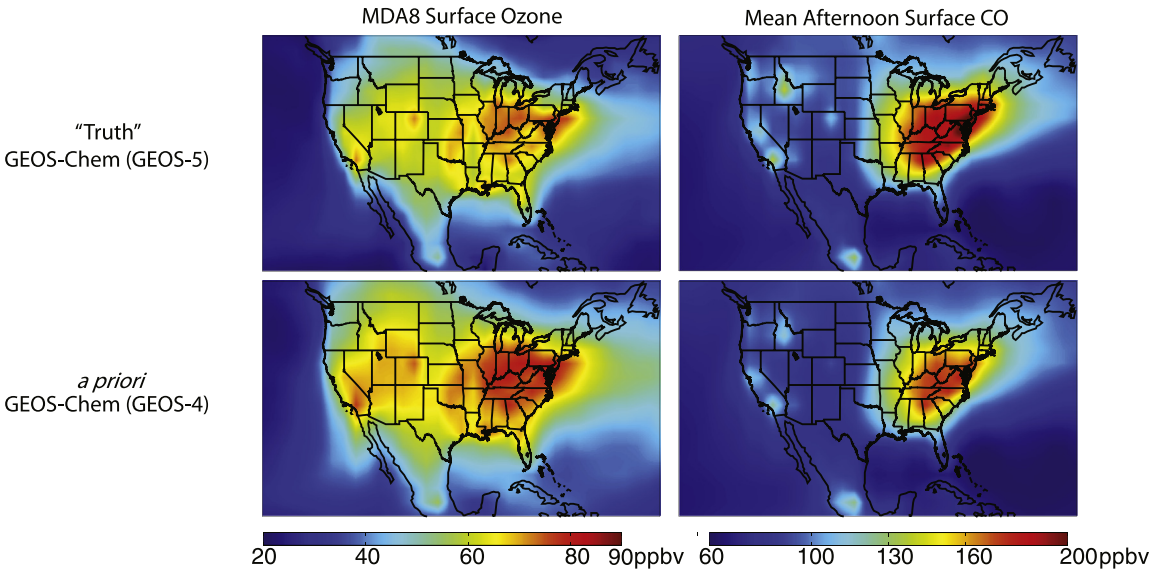

Fig. 1. Mean values of the maximum 8-h daily average (MDA8) ozone concentrations (left) and afternoon (1200–1700 local time) CO concentrations (right) for August 2006 in surface air. Top panels show values from the GEOS-5 model used as the "true" atmosphere in our OSSE. Bottom panels show values from the GEOS-4 model used as *a priori*.

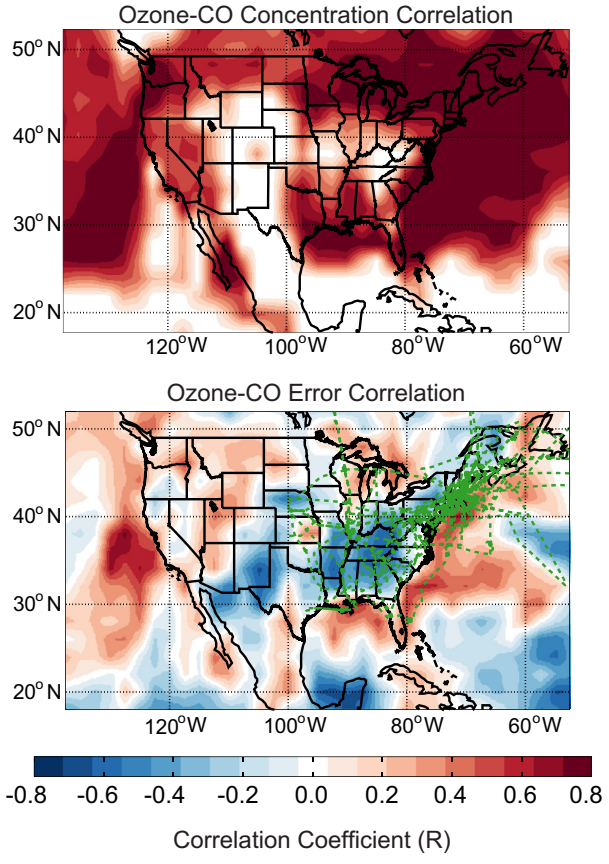

Fig. 2. Correlations of ozone and CO concentrations in the afternoon boundary layer in GEOS-4 (top) and corresponding error correlations for GEOS-4 compared to GEOS-5 (bottom). Concentrations are 0–2 km columns sampled hourly at 1200–1700 local time for August 2006. Flight tracks for the ICARTT aircraft campaign are overlain (dashed green line) for comparison with Fig. 3. (For interpretation of the references to color in this figure legend, the reader is referred to the web version of this article.)

Measurements from the ICARTT aircraft campaign over the eastern US and the western North Atlantic in July–August 2004 offer a test of these paired-model error correlation patterns. Ozone and CO concentrations were measured from two aircraft, the NASA DC-8 and the NOAA WP-3D (Singh et al., 2006; Fehsenfeld et al., 2006). A major objective of ICARTT was to better understand ozone production in the US boundary layer and the resulting outflow (Singh et al., 2006). Hudman et al. (2009) presented a detailed analysis of ozone–CO correlations in ICARTT to address this objective. Here we simulate the ICARTT observations using a nested continental-scale version of GEOS-Chem (Zhang et al., 2012) using GEOS-5 meteorological data with $1/2^\circ \times 2/3^\circ$ horizontal resolution ($\sim 50 \times 50$ km^2) in order to examine the correlations over different scales. In all cases we sample the model along the flight tracks and at the flight times (restricted to 0–2 km, 1200–1700 local time).

Fig. 3 **(top)** shows simulated and observed correlations of concentrations. Correlations are strongly positive, with consistent regression slopes (dO_3/dCO), as previously noted by Hudman et al. (2009). The model fails to reproduce urban and fire plumes with very high CO as these plumes are not resolved on the 50 km model scale.

The middle panel of Fig. 3 shows the model error (simulated − observed) in ozone concentration plotted against the corresponding model error in CO concentration for the afternoon boundary layer data. Strong positive error correlations are found in urban and fire plumes, diagnosed in the ICARTT data following Mao et al. (2013), but the model cannot resolve these plumes. Error correlations for the land and ocean data excluding plumes are plotted separately. We find that these model error correlations relative to the ICARTT data are similar to those in the paired-model analysis, with positive correlations over the ocean (continental outflow) and negative correlations over land (boundary layer depth). Land points east of 80oW (black symbols) show positive error correlations that likely reflect a dominant influence from continental outflow. Averaging the model and observations over a $2^\circ \times 2.5^\circ$ grid (Fig. 3, bottom panel) does not change the correlation statistics relative to the $1/2^\circ \times 2/3^\circ$ resolution.

The switch in sign of the ozone–CO error correlation between pollution plumes and the regional atmosphere complicates the use

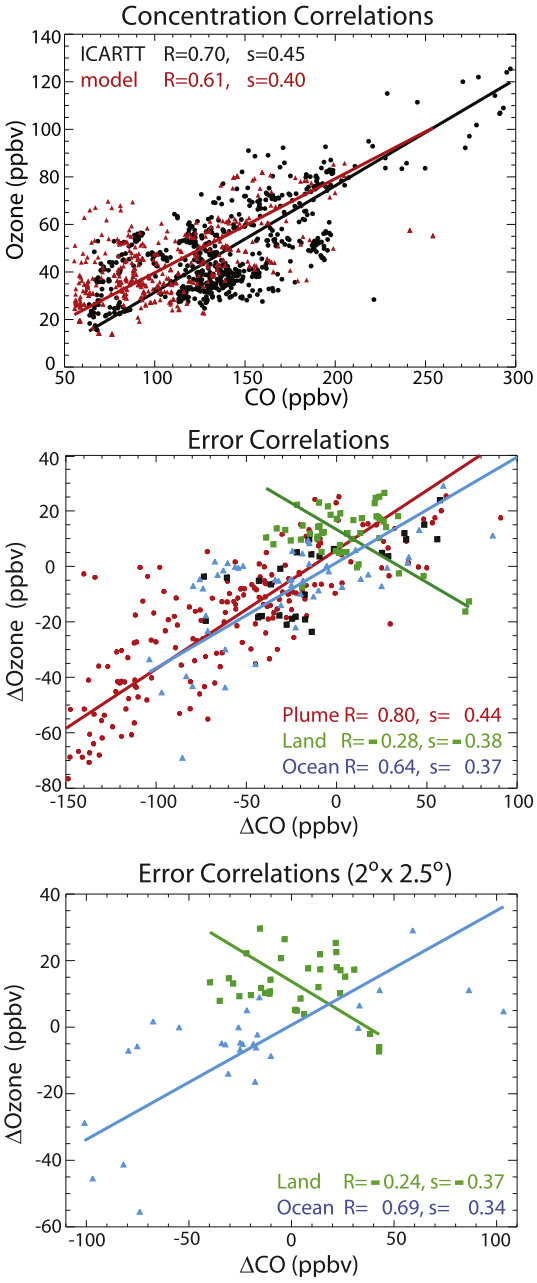

Fig. 3. Correlations between ozone and CO concentrations, and corresponding model error correlations, for afternoon boundary layer data (0–2 km, 12–17 local time) from the ICARTT aircraft campaign over the eastern US and western North Atlantic during July–August 2004 [Fehsenfeld et al., 2006; Singh et al., 2006]. ICARTT flight tracks are in Fig. 2. The top panel shows the correlation between concentrations in the observations and in the nested GEOS-Chem model with 1/2°x2/3° horizontal resolution as described in the text. The observations for individual flights are averaged over the model grid and the model is sampled at the time and location of the observations. The middle panel shows the error correlation for the differences Δ between GEOS-Chem values and ICARTT observations in pollution plumes, over land, and over ocean. The bottom panel shows the error correlations averaged over a 2°×2.5° grid. "Land" points in the middle and bottom panels are for the longitude range 100o-80oW sampled by ICARTT (Fig. 2). Other land points sampled by ICARTT (mainly in New England) are shown in black in the middle panel and are not used in correlative analyses. Correlation coefficients (R) and slopes of the reduced major-axis regression lines (s) are shown inset.

of ozone–CO error correlations in data assimilation. Because GEOS-Chem cannot resolve fine-scale pollution plumes, these must be excluded from the data assimilation. Such exclusion (justified by large model representation error) is standard when using atmospheric concentration data for source inversions (Palmer et al., 2003; Heald et al., 2004). Data assimilation with a finer-resolution model would need to use different error correlations statistics in fine-scale plumes and in regional air.

4. OSSE Design

We explore the benefit of using ozone–CO error correlations to improve data assimilation for surface ozone in GEOS-Chem by performing a paired-model OSSE with GEOS-5 as the "true" atmosphere and GEOS-4 as the forward model for data assimilation, as described in Section 3. Ozone–CO error correlations are geographically variable as shown in Fig. 2. Averaging kernel matrices for the satellite instruments (Fig. 4) are taken from the Natraj et al. (2011) theoretical study for GEO-CAPE ozone and from a sample NIR + TIR retrieval for MOPITT CO (Worden et al., 2010). We assume fixed averaging kernel matrices for the whole continental domain, acknowledging that there is in fact significant variability due to different surface albedos, temperatures and concentrations (Worden et al., 2013). Also shown in Fig. 4 are the degrees of freedom for signal (DOFS) below given pressure levels, estimated as the corresponding trace of the averaging kernel matrix and measuring the number of independent pieces of information in the retrieval (Rodgers, 2000). The CO averaging kernel matrix in Fig. 5 represents particularly favorable observing conditions for MOPITT, whose retrieval quality is often limited by large pixel size noise introduced by the changing view of the surface due to spacecraft motion during data scans (Deeter et al., 2011). It is however representative of the expected performance of GEO-CAPE, which will have a stationary field of regard (Fishman et al., 2012).

We generate synthetic geostationary observations of the "true" atmosphere for August 2006 by sampling the hourly daytime vertical profiles over land scenes in the North American domain with the averaging kernel matrices given in Fig. 4. We omit scenes with cloud fraction $>$ 0.3 (as given by the GEOS-5 meteorology). Gaussian random error is added to the synthetic observations to simulate spectral measurement error (instrument noise ε in eq. (1)) as given by Natraj et al. (2011) and Worden et al. (2010). As the GEO-CAPE footprint ($\sim$4 km) is much finer than the GEOS-Chem resolution used ($\sim$200 km), the instrument error is reduced by the square root of the number of observations available for the corresponding GEOS-Chem grid square.

We assimilate the synthetic observations of the "true" state into the forward model, as we would do with actual data, to correct the mismatch between the "true" and *a priori* states. We do this

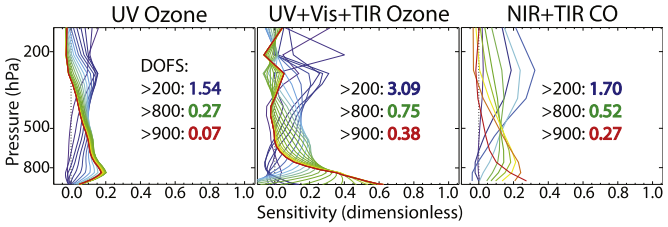

Fig. 4. Averaging kernel matrices for clear-sky satellite retrievals of ozone and CO assumed in this study. The averaging kernel matrices are from a GEO-CAPE theoretical study by Natraj et al., (2011) for ozone in the UV and in the UV + Vis + TIR, and from a sample retrieval of CO over land by MOPITT in the NIR + TIR [Worden et al., 2010]. Individual lines are the matrix rows corresponding to retrievals for individual vertical levels. The color gradient from red to blue corresponds to vertical levels ranging from the surface (red) to 200 hPa (blue). Inset are the degrees of freedom for signal (DOFS) for the atmospheric columns below 200, 800, and 900 hPa., estimated as the traces of the corresponding portions of the averaging kernel matrix. (For interpretation of the references to color in this figure legend, the reader is referred to the web version of this article.)

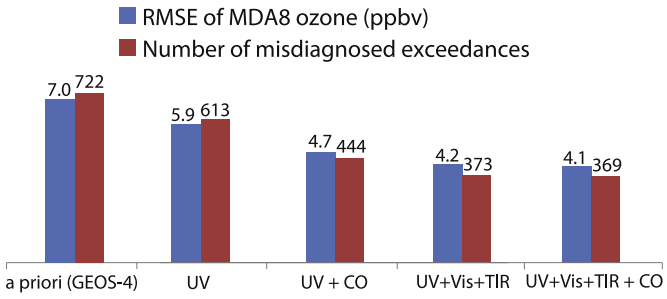

Fig. 5. Improved characterization of surface ozone air quality from assimilation of geostationary satellite observations of ozone and CO. Results are from OSSEs for August 2006 examining two error metrics: (1) the root mean square error (RMSE) of maximum daily 8-h average (MDA8) ozone over the contiguous US relative to the "true" state defined by the GEOS-5 simulation, and (2) the number of surface gridsquare-days where a NAAQS exceedance (MDA8 ozone >75 ppbv) is incorrectly diagnosed, either as a false positive or as a false negative. The error metrics from the GEOS-4 simulation without data assimilation (*a priori*) are compared to results from the assimilation of observations from a UV-only ozone instrument (UV) and a multispectral ozone instrument (UV + Vis + TIR), without and with joint assimilation of CO using ozone–CO error correlations (+CO).

sequentially by using a Kalman filter as described in Section 2, applying the filter iteratively at successive observation time steps to update the model state. The model error covariance matrix for each species ($\mathbf{S}_{a,O3}$ and $\mathbf{S}_{a,CO}$ in (4)) is assumed diagonal, and the diagonal terms are assumed constant and estimated from the Relative Residual Error (RRE) method (Palmer et al., 2003; Heald et al., 2004). This yields an altitude-independent error of 29% for O_3 (Zoogman et al., 2011) and 15% for CO (Heald et al., 2004).

5. Error reduction from ozone–CO joint assimilation

From the OSSE design in Section 4, we analyze the benefit of using ozone–CO model error correlations in a joint ozone–CO data assimilation system to constrain surface ozone concentrations over the contiguous US, as compared to an ozone-only data assimilation system. We focus on the maximum daily 8-h average (MDA8) ozone, which is the form of the NAAQS. We use two metrics to evaluate the assimilation results: (1) the Root Mean Square Error (RMSE) of MDA8 ozone relative to the "true" state, and (2) the number of incorrectly diagnosed NAAQS exceedances (MDA8 ozone >75 ppbv). These metrics are computed only over the US (25oN – 50oN, 125oW – 65oW, land only), but observations are assimilated over the entire North American domain (10oN – 60oN, 140oW – 40oW, land only). We conduct separate OSSEs for a UV-only and a UV + Vis + TIR ozone instrument, each with and without joint assimilation of CO, for a total of four OSSEs. Metrics (1) and (2) in the OSSE results are compared to the *a priori* model simulation without data assimilation.

Fig. 5 shows the data assimilation results. The RMSE for ozone without assimilation is 7.0 ppbv. For a UV-only ozone instrument, the joint ozone–CO assimilation reduces the RMSE by 33% as compared to a 16% reduction by the ozone-only assimilation. For a UV + Vis + TIR ozone instrument, the joint ozone–CO assimilation reduces the RMSE by 41% compared to a 39% reduction by the ozone-only assimilation. The CO assimilation has a major impact when the ozone instrument is UV-only, because the supplemental boundary information provided by the CO instrument is then important. The improvement from the joint assimilation is greatest in regions with strong error correlations and smallest over coastal regions where error correlations can switch sign over small spatial scales (Fig. 2) and are thus not robust. The UV + Vis + TIR ozone instrument has better sensitivity to the boundary layer than the CO instrument in Fig. 4, so that CO assimilation is of negligible benefit in that case. We see that joint assimilation of CO with a UV-only ozone instrument improves the representation of surface ozone concentrations in a manner that approaches the performance of the UV + Vis + TIR ozone instrument.

A goal for the GEO-CAPE mission is to improve the diagnosis and forecasting of exceedances of the ozone air quality standard. Over the US the "true" state of our OSSE experiences 422 gridsquare-days where MDA8 ozone exceeds 75 ppbv during August 2006. We see from Fig. 5 that the model *a priori* without data assimilation incurs 722 errors in diagnosing exceedances for that domain (either false positive or false negative). For a UV-only ozone instrument, the joint ozone–CO assimilation reduces the number of exceedance errors by 39%, as compared to a 15% reduction by the ozone-only assimilation. For the UV + Vis + TIR instrument, the ozone-only assimilation reduces the number of exceedance errors by 48% and the added CO assimilation has no significant benefit. These statistics and their interpretation are similar to the RMSE results.

6. Conclusions

We explored the value of combining geostationary satellite data for ozone and CO in a joint ozone–CO data assimilation system to inform ozone air quality. The idea is that a multispectral (NIR + TIR) CO instrument with sensitivity in the boundary layer can help to constrain surface ozone through correlation of ozone and CO errors in the chemical transport model (CTM) used for data assimilation. We implemented the joint assimilation in an Observing System Simulation Experiment (OSSE) of the planned NASA GEO-CAPE geostationary mission over North America. We considered two possibilities for the ozone instrument, UV-only or multispectral (UV + Vis + TIR).

Proper characterization of model error correlations between ozone and CO in the boundary layer is critical for the joint assimilation. These error correlations can be very different from the correlations between the concentrations themselves. We generated them by a paired-model method using GEOS-Chem CTM simulations with 2°×2.5° horizontal resolution driven by different assimilated meteorological data sets (GEOS-4 and GEOS-5) for the same August 2006 period. Results indicate positive ozone–CO error correlations in continental outflow regions, reflecting common horizontal transport. However, error correlations are negative over much of the US, particularly in the Midwest (80° – 100° W), even though the concentrations themselves are positively correlated. These negative error correlations reflect opposite sensitivities of ozone and CO to model error in boundary layer depth.

We tested the ozone–CO error correlation patterns from the paired-model method by using ICARTT aircraft observations in the boundary layer over the eastern US and western North Atlantic during July–August 2004. Strong and consistent positive correlations are found between ozone and CO concentrations in the observations and in a nested GEOS-Chem simulation (1/2°× 2/3° horizontal resolution). Error correlations between the nested GEOS-Chem simulation and the ICARTT observations are strongly positive in subgrid pollution plumes and in continental outflow over the ocean, but negative over land outside of plumes, consistent with the paired-model statistics. GEOS-Chem is too coarse to resolve pollution plumes and so these must be excluded from the data assimilation. A finer-scale data assimilation system to resolve these plumes would need to account for the difference in error correlation between the concentrated plumes (with positive error correlation determined by common dilution of ozone and CO) and regional air (where boundary layer depth drives a negative error correlation).

Our OSSE results indicate that adding multispectral CO measurements in a joint assimilation with UV ozone observations from geostationary orbit could provide significant improvement to constraints on surface ozone air quality. However, we find no significant benefit if ozone is measured by a multispectral UV + Vis + TIR instrument that has higher boundary layer sensitivity than the CO instrument. Adding a CO measurement capability to a UV ozone observing system provides constraints on surface ozone approaching those from a UV + Vis + TIR ozone observing system, if the ozone–CO error correlation statistics can be well characterized. We considered here a multispectral CO instrument since this is the design of GEO-CAPE, but a NIR-only instrument measuring the CO column may provide comparable benefit if most of the CO variability is in the boundary layer. This would need to be investigated in further OSSE work.

Our study used the same pair of models to compute the ozone–CO error correlations and to simulate the data assimilation procedure, which may overestimate the information provided by the error correlations. The OSSE could be improved through the use of a third independent model or the "paired-forecast" method (as in Wang et al., 2009). It would obviously be best to derive the error correlations from observations, but aircraft observations are too sparse and current satellite observations of ozone have little boundary layer sensitivity. Future implementation of this method will benefit from satellite observations that have some sensitivity to boundary layer ozone (but less than concurrent sensitivity to boundary layer CO) to construct the spatial pattern of error correlations at the appropriate resolution for data assimilation. Observations can also be used to test the error correlation patterns derived from model analyses, as we did here with ICARTT aircraft data.

Acknowledgments

This work was supported by the NASA Atmospheric Composition and Modeling Program and by a NASA Earth and Space Science Fellowship to Peter Zoogman.

References

Bak, J., Kim, J.H., Liu, X., Chance, K., Kim, J., 2013. Evaluation of ozone profile and tropospheric ozone retrievals from GEMS and OMI spectra. Atmos. Measur. Tech. 6, 239–249.

Beer, R., 2006. TES on the aura mission: scientific objectives, measurements, and analysis overview. IEEE Trans. Geosci. Rem. Sens. 44, 1102–1105.

Bey, I., Jacob, D., Yantosca, R., Logan, J., Field, B., Fiore, A., Li, Q., Liu, H., Mickley, L., Schultz, M., 2001. Global modeling of tropospheric chemistry with assimilated meteorology: model description and evaluation. J. Geophys. Res.-Atmos. 106, 23073–23095.

Bloom, S., da Silva, A., Dee, D., Bosilovich, M., Chern, J., Pawson, S., Schubert, S., Sienkiewicz, M., Stajner, I., Tan, W., Wu, M., 2005. The Goddard Earth Observing Data Assimilation System, GEOS DAS Version 4.0.3: Documentation and Validation. NASA Tech. Rep. 104606.

Bovensmann, H., Burrows, J., Buchwitz, M., Frerick, J., Noel, S., Rozanov, V., Chance, K., Goede, A., 1999. SCIAMACHY: mission objectives and measurement modes. J. Atmos. Sci. 56, 127–150.

Chin, M., Jacob, D., Munger, J., Parrish, D., Doddridge, B., 1994. Relationship of ozone and carbon-monoxide over north-america. J. Geophys. Res.-Atmos. 99, 14565–14573.

Clerbaux, C., Boynard, A., Clarisse, L., George, M., Hadji-Lazaro, J., Herbin, H., Hurtmans, D., Pommier, M., Razavi, A., Turquety, S., Wespes, C., Coheur, P., 2009. Monitoring of atmospheric composition using the thermal infrared IASI/MetOp sounder. Atmos. Chem. Phys. 9, 6041–6054.

Cuesta, J., Eremenko, M., Liu, X., Dufour, G., Cai, Z., Höpfner, M., von Clarmann, T., Sellitto, P., Foret, G., Gaubert, B., Beekmann, M., Orphal, J., Chance, K., Spurr, R., Flaud, J.-M., 2013. Satellite observation of lowermost tropospheric ozone by multispectral synergism of IASI thermal infrared and GOME-2 ultraviolet measurements. Atmos. Chem. Phys. Discuss 13, 2955–2995.

Dawson, J.P., Adams, P.J., Pandis, S.N., 2007. Sensitivity of ozone to summertime climate in the eastern USA: A modeling case study. Atmos. Environ. 41, 1494–1511.

Deeter, M.N., Worden, H.M., Gille, J.C., Edwards, D.P., Mao, D., Drummond, J.R., 2011. MOPITT multispectral CO retrievals: origins and effects of geophysical radiance errors. J. Geophys. Res.-Atmos. 116, D15303.

Edwards, D.P., Arellano Jr., A.F., Deeter, M.N., 2009. A satellite observation system simulation experiment for carbon monoxide in the lowermost troposphere. J. Geophys. Res.-Atmos. 114, D14304.

Fehsenfeld, F.C., Ancellet, G., Bates, T.S., Goldstein, A.H., Hardesty, R.M., Honrath, R., Law, K.S., Lewis, A.C., Leaitch, R., McKeen, S., Meagher, J., Parrish, D.D., Pszenny, A.A.P., Russell, P.B., Schlager, H., Seinfeld, J., Talbot, R., Zbinden, R., 2006. International consortium for atmospheric research on transport and transformation (ICARTT): north america to europe – overview of the 2004 summer field study. J. Geophys. Res.-Atmos. 111, D23S01.

Fishman, J., Iraci, L.T., Al-Saadi, J., Chance, K., Chavez, F., Chin, M., Coble, P., Davis, C., DiGiacomo, P.M., Edwards, D., Eldering, A., Goes, J., Herman, J., Hu, C., Jacob, D.J., Jordan, C., Kawa, S.R., Key, R., Liu, X., Lohrenz, S., Mannino, A., Natraj, V., Neil, D., Neu, J., Newchurch, M., Pickering, K., Salisbury, J., Sosik, H., Subramaniam, A., Tzortziou, M., Wang, J., Wang, M., 2012. The United States' next generation of atmospheric composition and coastal ecosystem measurements NASA's geostationary coastal and air pollution events (GEO-CAPE) mission. Bull. Am. Meteorol. Soc. 93, 1547.

Fu, D., Worden, J.R., Liu, X., Kulawik, S.S., Bowman, K.W., Natraj, V., 2013. Characterization of ozone profiles derived from aura TES and OMI radiances. Atmos. Chem. Phys. 13, 3445–3462.

Heald, C., Jacob, D., Jones, D., Palmer, P., Logan, J., Streets, D., Sachse, G., Gille, J., Hoffman, R., Nehrkorn, T., 2004. Comparative inverse analysis of satellite (MOPITT) and aircraft (TRACE-P) observations to estimate asian sources of carbon monoxide. J. Geophys. Res.-Atmos. 109, D23306.

Hegarty, J., Mao, H., Talbot, R., 2010. Winter- and summertime continental influences on tropospheric O-3 and CO observed by TES over the western north atlantic ocean. Atmos. Chem. Phys. 10, 3723–3741.

Hegarty, J., Mao, H., Talbot, R., 2009. Synoptic influences on springtime tropospheric O-3 and CO over the North American export region observed by TES. Atmos. Chem. Phys. 9, 3755–3776.

Hudman, R.C., Murray, L.T., Jacob, D.J., Turquety, S., Wu, S., Millet, D.B., Avery, M., Goldstein, A.H., Holloway, J., 2009. North american influence on tropospheric ozone and the effects of recent emission reductions: constraints from ICARTT observations. J. Geophys. Res.-Atmos. 114, D07302.

Ingmann, P., Veihelmann, B., Langen, J., Lamarre, D., Stark, H., Courreges-Lacoste, G.B., 2012. Requirements for the GMES atmosphere service and ESA's implementation concept: sentinels-4/-5 and-5p. Rem. Sens. Environ. 120, 58–69.

Khattatov, B., Lamarque, J., Lyjak, L., Menard, R., Levelt, P., Tie, X., Brasseur, G., Gille, J., 2000. Assimilation of satellite observations of long-lived chemical species in global chemistry transport models. J. Geophys. Res.-Atmos. 105, 29135–29144.

Kim, P.S., Jacob, D.J., Liu, X., Warner, J.X., Yang, K., Chance, K., 2013. Global ozone–CO correlations from OMI and AIRS: constraints on tropospheric ozone sources. Atmos. Chem. Phys 13, 9321–9335.

Kopacz, M., Jacob, D.J., Henze, D.K., Heald, C.L., Streets, D.G., Zhang, Q., 2009. Comparison of adjoint and analytical bayesian inversion methods for constraining asian sources of carbon monoxide using satellite (MOPITT) measurements of CO columns. J. Geophys. Res.-Atmos. 114, D04305.

Liu, J., Logan, J.A., Murray, L.T., Pumphrey, H.C., Schwartz, M.J., Megretskaia, I.A., 2013. Transport analysis and source attribution of seasonal and interannual variability of CO in the tropical upper troposphere and lower stratosphere. Atmos. Chem. Phys. 13, 129–146.

Liu, J., Logan, J.A., Jones, D.B.A., Livesey, N.J., Megretskaia, I., Carouge, C., Nedelec, P., 2010a. Analysis of CO in the tropical troposphere using aura satellite data and the GEOS-chem model: insights into transport characteristics of the GEOS meteorological products. Atmos. Chem. Phys. 10, 12207–12232.

Liu, X., Bhartia, P.K., Chance, K., Spurr, R.J.D., Kurosu, T.P., 2010b. Ozone profile retrievals from the ozone monitoring instrument. Atmos. Chem. Phys. 10, 2521–2537.

Liu, X., Chance, K., Sioris, C., Kurosu, T., Spurr, R., Martin, R., Fu, T., Logan, J., Jacob, D., Palmer, P., Newchurch, M., Megretskaia, I., Chatfield, R., 2006. First directly retrieved global distribution of tropospheric column ozone from GOME: comparison with the GEOS-CHEM model. J. Geophys. Res.-Atmos. 111, D02308.

Mao, J., Paulot, F., Jacpb, D.J., Cohen, R.C., Crounse, J.D., Wennberg, P.O., Keller, C.A., Hudman, R.C., Barkley, M.P., Horowitz, L.W., 2013. Ozone and organic nitrates over the eastern United States: sensitivity to isoprene chemistry. J. Geophys. Res (submitted for publication).

Martin, R.V., 2008. Satellite remote sensing of surface air quality. Atmos. Environ. 42, 7823–7843.

Mitovski, T., Folkins, I., Martin, R.V., Cooper, M., 2012. Testing convective transport on short time scales: comparisons with mass divergence and ozone anomaly patterns about high rain events. J. Geophys. Res.-Atmos. 117, D02109.

National Research Council, 2007. Earth Science and Applications from Space: National Imperatives for the Next Decade and Beyond. The National Academies Press, Washington, DC.

Natraj, V., Liu, X., Kulawik, S., Chance, K., Chatfield, R., Edwards, D.P., Eldering, A., Francis, G., Kurosu, T., Pickering, K., Spurr, R., Worden, H., 2011. Multi-spectral sensitivity studies for the retrieval of tropospheric and lowermost tropospheric ozone from simulated clear-sky GEO-CAPE measurements. Atmos. Environ. 45, 7151–7165.

Ott, L.E., Bacmeister, J., Pawson, S., Pickering, K., Stenchikov, G., Suarez, M., Huntrieser, H., Loewenstein, M., Lopez, J., Xueref-Remy, I., 2009. Analysis of convective transport and parameter sensitivity in a single column version of the goddard earth observation system, version 5, general circulation model. J. Atmos. Sci. 66, 627–646.

Palmer, P.I., Suntharalingam, P., Jones, D.B.A., Jacob, D.J., Streets, D.G., Fu, Q., Vay, S.A., Sachse, G.W., 2006. Using CO_2: CO correlations to improve inverse analyses of carbon fluxes. J. Geophys. Res.-Atmos. 111, D12318.

Palmer, P., Jacob, D., Fiore, A., Martin, R., Chance, K., Kurosu, T., 2003. Mapping isoprene emissions over North America using formaldehyde column observations from space. J. Geophys. Res.-Atmos. 108, 4180.

Parrington, M., Jones, D.B.A., Bowman, K.W., Horowitz, L.W., Thompson, A.M., Tarasick, D.W., Witte, J.C., 2008. Estimating the summertime tropospheric ozone distribution over North America through assimilation of observations from the tropospheric emission spectrometer. J. Geophys. Res.-Atmos. 113, D18307.

Parrish, D., Trainer, M., Holloway, J., Yee, J., Warshawsky, M., Fehsenfeld, F., Forbes, G., Moody, J., 1998. Relationships between ozone and carbon monoxide at surface sites in the north Atlantic region. J. Geophys. Res.-Atmos. 103, 13357–13376.

Parrish, D., Holloway, J., Trainer, M., Murphy, P., Forbes, G., Fehsenfeld, F., 1993. Export of north-american ozone pollution to the North-Atlantic ocean. Science 259, 1436–1439.

Rienecker, M.M., Suarez, M.J., Todling, R., Bacmeister, J., Takacs, L., Liu, H.-C., Gu, W., Sienkiewicz, M., Koster, R.D., Gelaro, R., Stajner, I., Nielsen, J.E., 2008. NASA GSFC Technical Report Series on Global Modeling and Data Assimilation, NASA/TM-2007-104606. The GEOS-5 Data Assimilation System—documentation of Versions 5.0.1, 5.1.0, and 5.2.0, vol. 27, p. 92.

Rodgers, C.D., 2000. Inverse Methods for Atmospheric Sounding. World Scientific, River Edge, New Jersey,.

Singh, H.B., Brune, W.H., Crawford, J.H., Jacob, D.J., Russell, P.B., 2006. Overview of the summer 2004 intercontinental chemical transport experiment - north america (INTEX-A). J. Geophys. Res.-Atmos. 111, D24S01.

United States Environmental Protection Agency, 2012. Welfare Risk and Exposure Assessment for Ozone.

Voulgarakis, A., Telford, P.J., Aghedo, A.M., Braesicke, P., Faluvegi, G., Abraham, N.L., Bowman, K.W., Pyle, J.A., Shindell, D.T., 2011. Global multi-year O-3-CO correlation patterns from models and TES satellite observations. Atmos. Chem. Phys. 11, 5819–5838.

Wang, H., Jacob, D.J., Kopacz, M., Jones, D.B.A., Suntharalingam, P., Fisher, J.A., Nassar, R., Pawson, S., Nielsen, J.E., 2009. Error correlation between CO_2 and CO as constraint for CO_2 flux inversions using satellite data. Atmos. Chem. Phys. 9, 7313–7323.

Worden, H.M., Deeter, M.N., Frankenberg, C., George, M., Nichitiu, F., Worden, J., Aben, I., Bowman, K.W., Clerbaux, C., Coheur, P.F., de Laat, A.T.J., Detweiler, R., Drummond, J.R., Edwards, D.P., Gille, J.C., Hurtmans, D., Luo, M., Martinez-Alonso, S., Massie, S., Pfister, G., Warner, J.X., 2013. Decadal record of satellite carbon monoxide observations. Atmos. Chem. Phys. 13, 837–850.

Worden, H.M., Deeter, M.N., Edwards, D.P., Gille, J.C., Drummond, J.R., Nedelec, P., 2010. Observations of near-surface carbon monoxide from space using MOPITT multispectral retrievals. J. Geophys. Res.-Atmos. 115, D18314.

Zhang, L., Jacob, D.J., Knipping, E.M., Kumar, N., Munger, J.W., Carouge, C.C., van Donkelaar, A., Wang, Y.X., Chen, D., 2012. Nitrogen deposition to the united states: distribution, sources, and processes. Atmos. Chem. Phys. 12, 4539–4554.

Zhang, L., Jacob, D.J., Liu, X., Logan, J.A., Chance, K., Eldering, A., Bojkov, B.R., 2010. Intercomparison methods for satellite measurements of atmospheric composition: application to tropospheric ozone from TES and OMI. Atmos. Chem. Phys. 10, 4725–4739.

Zhang, L., Jacob, D.J., Kopacz, M., Henze, D.K., Singh, K., Jaffe, D.A., 2009. Intercontinental source attribution of ozone pollution at western US sites using an adjoint method. Geophys. Res. Lett. 36, L11810.

Zhang, L., Jacob, D.J., Bowman, K.W., Logan, J.A., Turquety, S., Hudman, R.C., Li, Q., Beer, R., Worden, H.M., Worden, J.R., Rinsland, C.P., Kulawik, S.S., Lampel, M.C., Shephard, M.W., Fisher, B.M., Eldering, A., Avery, M.A., 2006. Ozone–CO correlations determined by the TES satellite instrument in continental outflow regions. Geophys. Res. Lett. 33, L18804.

Zoogman, P., Jacob, D.J., Chance, K., Zhang, L., Le Sager, P., Fiore, A.M., Eldering, A., Liu, X., Natraj, V., Kulawik, S.S., 2011. Ozone air quality measurement requirements for a geostationary satellite mission. Atmos. Environ. 45, 7143–7150.